Theory of the surface magnetization profile and the low-energy, spin-polarized, inelastic electron scattering off insulating ferromagnets at finite T

Silvia Selzer*
International Centre for Theoretical Physics, Trieste, Italy
and Scuola Internazionale Superiore di Studi Avanzati, Trieste, Italy

Norberto Majlis*
Scuola Internazionale Superiore di Studi Avanzati, Trieste, Italy
(Received 26 June 1981)

A semi-infinite Heisenberg ferromagnet with nearest-neighbor exchange interactions is studied at finite T. The Green functions are evaluated by extending the random-phase approximation to consider the spatial variation of the layer magnetization, which is calculated self-consistently at all temperatures up to T_c. Results for an fcc lattice with a (111) surface turn out qualitatively similar to previous results for a sc lattice with a (100) surface. In both cases the surface has the same T_c as the bulk, irrespective of the difference between surface and bulk exchange constants. A survey is presented of a continued fraction representation for the Green functions in the mixed local-Bloch basis for the spin operators, related to the transfer-matrix formalism, which allows explicit evaluation of the diagonal Green function at each layer. The calculation was performed by truncating the spatial variation of the magnetization, at any T, at the third layer of the lattice. The currently available intense sources of spin-polarized electrons offer a possibility of obtaining quantitative information on the surface parameters. The differential cross section for low-energy electron scattering is calculated for the fcc lattice at zero momentum transfer. The curves show resonances near one or both ends of the bulk magnon energy band, depending on the surface exchange parameters.

I. INTRODUCTION

The recent development of efficient sources of spin-polarized electrons[1] has stimulated the study of the surface properties of magnetic systems.

Both elastic and inelastic scattering of low-energy electrons off insulating magnetic samples can afford very detailed information on the surface magnetic structure[2] and on the spectrum of magnetic excitations, whether surface localized or bulk.[3,4] This is because low-energy electrons, with energies up to 150 eV, do not penetrate further than one or two atomic layers into the crystal, being, in consequence, an invaluable probe of the surface properties.

In this paper we present what, to our knowledge, is the first calculation in which are simultaneously obtained in a self-consistent way, the layer magnetization profile, the bulk magnetization, and the spectrum of bulk and surface magnetic excitations for any spin S and for all temperatures T, up to T_c, of an isotropic Heisenberg semi-infinite ferromagnet with nearest-neighbor exchange interactions.

We adopt the Green function formalism of Zubarev[5] and use the mixed local-Bloch representation, as introduced in the context of surface magnetism by De Wames and Wolfram.[4]

The Green functions are evaluated in the random-phase approximation (RPA) by the simultaneous self-consistent evaluation of the layer magnetization at the surface ($n=0$) plane, and the next inner plane ($n=1$), assuming for simplicity that the bulk magnetization value is reached at $n=2$. We have already briefly reported elsewhere[6] on our RPA results for the surface magnetization in simple cubic ferromagnets with a (100) surface. We now present the method of calculation of the Green functions (Sec. II) for the simple cubic and the fcc semi-infinite lattice structures, expressing them as continued fractions.

Since the bulk magnetization is a necessary ingredient, we calculate it also in the RPA, following the work of Tahir-Kheli and Ter Haar.[7] An RPA calculation of the self-consistent magnetization profile for a twenty-layer thin film, including exchange and single-ion anisotropy, was performed by Diep-The-Hung *et al.*,[8] for $S=\frac{1}{2}$ in the sc and bcc structures. We discuss our results for the magnetization profile, the surface magnetization and the surface magnon dispersion relations in Sec. III.

Section IV is devoted to indicate how these results can be applied to the calculation of the differential cross section for inelastic scattering of low-energy electrons. Calculations thereof at low temperatures have already been performed (see Ref. 9 and references therein).

In a similar calculation for a metallic ferromagnet, Saldaña and Helman[10] used pseudopotential results for the bulk magnetization, although they recognize that the surface magnetization should be used instead. We consider, following previous treatments of this problem,[3,9] that electrons interact only with the surface spin layer, and that their interactions with the spin system is of the contact form proposed by De Gennes and Friedel.[11]

In the fcc case with a (111) surface, numerical results are specialized to the case of EuO with $S=\frac{7}{2}$, since we believe it should be a good candidate for eventual comparison with experiments, but it is found that no qualitative changes arise for other values of S.

II. SELF-CONSISTENT CALCULATION OF THE MAGNETIZATION PROFILE

We consider a semi-infinite, insulating ferromagnetic crystal described by the Heisenberg Hamiltonian

$$H=-\sum_{l\neq m} I_{lm}\vec{S}_l\cdot\vec{S}_m \ , \tag{1}$$

where the exchange constants between nearest neighbors are: $I_{\parallel}$ for bonds in the plane of the surface, $I_{\perp}$ for bonds between the surface and the second plane, and I for all other bonds. We calculate Zubarev's Green functions[5]

$$G^{+}_{lm}(t-t_0)\equiv\langle\langle S_l^{+};S_m^{-}\rangle\rangle \equiv -i\Theta(t-t_0)\langle[S_l^{+}(t),S_m^{-}(t_0)]\rangle \ . \tag{2}$$

We use a generalization of the RPA decoupling[6,8] that allows for spatial variation of $\langle S_g^z\rangle$ over an arbitrary number of planes parallel to the surface:

$$\langle\langle S_g^z S_f^{+};S_l^{-}\rangle\rangle \simeq \langle S_g^z\rangle\langle\langle S_f^{+};S_l^{-}\rangle\rangle \ . \tag{3}$$

The subindices denote lattice sites. The statistical mean $\langle S_g^z\rangle$ only depends on the position of the plane parallel to the surface. We assume the magnetization to be parallel to the surface in order not to consider demagnetizing fields.

The resulting equations of motion are

$$\left[\omega\delta_{gl}-2\sum_f I_{fg}\langle S_f^z\rangle\right]G_{gl}(\omega) = \frac{1}{\pi}\delta_{gl}\langle S_g^z\rangle-2\sum_f I_{fg}G_{fl}(\omega)\langle S_f^z\rangle \ . \tag{4}$$

These equations are identical to those used in Ref. 8 for a finite number of layers.

A. Simple cubic ferromagnet with nearest-neighbor interactions

It is convenient[4,6,8] to decompose the lattice vector $\vec{f}\equiv(\vec{f}_{\parallel},f_3)$ and to define the Fourier transform of (4) with respect to the "parallel" components $\vec{f}_{\parallel}\equiv(f_x,f_z)$:

$$G_{fg}(\omega)=\frac{1}{N_s}\sum_{\vec{k}_{\parallel}}\tilde{G}_{f_3g_3}(\vec{k}_{\parallel},\omega)\exp[i\vec{k}_{\parallel}\cdot(\vec{f}_{\parallel}-\vec{g}_{\parallel})] \ , \tag{5}$$

where we have taken advantage of the translation symmetry parallel to the surface

$$I_{fg}\equiv I_{\vec{f}_{\parallel}-\vec{g}_{\parallel};f_3g_3} =\frac{1}{N_s}\sum_{\vec{k}_{\parallel}}\tilde{I}_{f_3g_3}(\vec{k}_{\parallel})\exp[i\vec{k}_{\parallel}\cdot(\vec{f}_{\parallel}-\vec{g}_{\parallel})] \ . \tag{6}$$

We obtain the matrix equation

$$2\pi(\nu\mathbb{1}-\underline{H}^{\rm eff})\underline{g}=2\pi\,\underline{\Omega}\,\underline{g}=\underline{\sigma} \tag{7a}$$

or

$$\underline{g}=\frac{1}{2\pi(\nu\mathbb{1}-\underline{H}^{\rm eff})}\sigma \ , \tag{7b}$$

where

$$H^{\rm eff}_{nm}(\vec{k}_{\parallel})=\delta_{nm}[\epsilon_{\vec{k}_{\parallel}}(m)\sigma_m+\epsilon_{\perp}(m,m+1)\sigma_{m+1}+\epsilon_{\perp}(m,m-1)\sigma_{m-1}] -[\epsilon_{\vec{k}_{\parallel}}(n)\delta_{nm}+\epsilon_{\perp}(n,m)\delta_{n,m+1}+\epsilon_{\perp}(n,m)\delta_{n,m-1}]\sigma_m \ , \tag{8a}$$

defining the dimensionless variables:

$$\epsilon_{\vec{k}_{\parallel}}(n)=4\gamma_0(\vec{k}_{\parallel})\begin{cases}I_{\parallel}/I, & n=0\\ 1, & \text{otherwise}\end{cases} \ , \quad \gamma_0(\vec{k}_{\parallel})=\tfrac{1}{2}(\cos k_x a+\cos k_z a) \ , \quad \epsilon_{\perp}(n,m)=\begin{cases}I_{\perp}/I, & n \text{ or } m=0\\ 1, & \text{otherwise}\end{cases} \ ,$$

$$\sigma_m=\langle S_m^z\rangle/\langle S_{\rm vol}^z\rangle \ , \quad \underline{g}\equiv I\underline{G} \ . \tag{8b}$$

We take for simplicity $\sigma_m=1$ for $m\geq 2$; ν is the angular frequency in units of $2I\langle S_{\rm vol}^z\rangle$.

The matrix

$$\underline{\Omega}\equiv\nu\mathbb{1}-\underline{H}^{\rm eff} \tag{9}$$

is

$$\underline{\Omega}=\begin{pmatrix} 2t+\alpha_{00} & \beta_{01} & 0 & 0 & \cdot & \cdot & \cdot \\ \beta_{10} & 2t+\alpha_{11} & \beta_{12} & 0 & \cdot & \cdot & \cdot \\ 0 & \beta_{21} & 2t+\alpha_{22} & 1 & 0 & \cdot & \cdot \\ 0 & 0 & 1 & 2t & 1 & \cdot & \cdot \\ 0 & 0 & 0 & 1 & 2t & 1 & \cdot \\ \cdot & \cdot & \cdot & \cdot & \cdot & \cdot & \cdot \end{pmatrix} , \quad (10)$$

where, calling $I_{\perp}/I=\epsilon_{\perp}$ and $I_{\parallel}/I=\epsilon_{\parallel}$, we have

$$\Omega_{\substack{nn \\ n\to\infty}} \to 2t \equiv \nu - 2 - 4[1-\gamma_0(\vec{k}_{\parallel})] , \quad (11)$$

$$\left.\begin{aligned} &\alpha_{00}=2-\sigma_1\epsilon_{\perp}+4(1-\epsilon_{\parallel}\sigma_0)[1-\gamma_0(\vec{k}_{\parallel})] \\ &\alpha_{11}=1-\sigma_0\epsilon_{\perp}+4(1-\sigma_1)[1-\gamma_0(\vec{k}_{\parallel})] \\ &\alpha_{22}=1-\sigma_1 \\ &\beta_{01}=\sigma_0\epsilon_{\perp},\quad \beta_{10}=\sigma_1\epsilon_{\perp},\quad \beta_{12}=\sigma_1,\quad \beta_{21}=1 \end{aligned}\right\} . \quad (12)$$

Since $\underline{\Omega}$ is a tri-diagonal it is easy to calculate directly the elements of Ω^{-1}.

Calling $D_N \equiv \det\underline{\Omega}$ and D_{N-p} the determinant obtained from D_N, deleting the first p rows and columns, we get

$$(\Omega^{-1})_{00}=\frac{D_{N-1}}{D_N} , \quad (13)$$

where

$$\left.\begin{aligned} &D_N=(2t+\alpha_{00})D_{N-1}-\beta_{10}\beta_{01}D_{N-2} \\ &D_{N-1}=(2t+\alpha_{11})D_{N-2}-\beta_{12}\beta_{21}D_{N-3} \\ &\quad\vdots \\ &D_{N-p}=2tD_{N-p-1}-D_{N-p-2} \\ &\quad\vdots \end{aligned}\right\} . \quad (14)$$

For $p>2$ all determinants D_{N-p} have the nonperturbed form:

$$\begin{vmatrix} 2t & 1 & 0 & \cdots \\ 1 & 2t & 1 & \cdots \\ 0 & 1 & 2t & \cdots \\ \cdot & \cdot & \cdot & \cdots \\ \cdot & \cdot & \cdot & \cdots \end{vmatrix} . \quad (15)$$

These determinants, also found by De Wames and Wolfram[4] in the solution of the equations of motion for the operator S_l^+ in the Holstein-Primakoff approximation, are the associate Tchebishev polynomials of the first kind $U_{N-p}(t)$

$$D_{N-p}(t)\equiv U_{N-p}(t) .$$

Using recurrence formulas (14) one can rewrite (13) as

$$(\Omega^{-1})_{00}=\frac{1}{2t+\alpha_{00}-\beta_{10}\beta_{01}(D_N/D_{N-1})} . \quad (16)$$

We substitute again D_{N-1} in terms of D_{N-2} and D_{N-3} and so on, until we arrive at a ratio of two unperturbed determinants of the form of (15) for $p>2$.

This ratio can now be written as

$$\frac{D_{N-p-1}}{D_{N-p}}=\frac{U_{N-p-1}}{U_{N-p}}=\frac{1}{2t-U_{N-p-1}/U_{N-p}} . \quad (17)$$

Taking now the limit $(N-p)\to\infty$ we define

$$\xi(t)=\lim_{(N-p)\to\infty}\frac{U_{N-p-1}(t)}{U_{N-p}(t)} . \quad (18a)$$

Equation (18a) can be written in the limit $N-p\to\infty$

$$\xi(t)=\frac{1}{2t-(1/2t-\cdots)} \quad (18b)$$

or

$$\xi=\frac{1}{2t-\xi} \quad (19)$$

equivalent to

$$\xi^2-2t\xi+1=0 \quad (20)$$

or

$$\xi+\xi^{-1}=2t . \quad (21)$$

Therefore, for a semi-infinite system, $N\to\infty$, $(\Omega^{-1})_{00}$, and $(\Omega^{-1})_{11}$ take the form

$$(\Omega^{-1})_{00}=\frac{1}{2t+\alpha_{00}-\beta_{10}\beta_{01}\Big/\left(2t+\alpha_{11}-\dfrac{\beta_{12}\beta_{21}}{2t+\alpha_{22}-\xi}\right)} , \quad (22a)$$

$$(\Omega^{-1})_{11}=\frac{1}{2t+\alpha_{11}-\dfrac{\beta_{10}\beta_{01}}{2t+\alpha_{00}}-\dfrac{\beta_{12}\beta_{21}}{2t+\alpha_{22}-\xi}} . \quad (22b)$$

In order to interpret the physical meaning of the parameter $\xi(t)$ [Eq. (18a)] we shall need the analytic continuation of $U_n(t)$ to the complex t plane.

For t real, and $|t|<1$, we define $t\equiv\cos\theta$, and we can use the representation

$$U_n(\cos\theta)=\frac{\sin(n+1)\theta}{\sin\theta} , \quad (23)$$

$U_n(t)$ is an n-degree polynomial in t. All its roots are contained in $|t|\leq 1$. In this interval of t, ξ is complex, since from (20):

$$\xi(t)=t\pm i(1-t^2)^{1/2}=e^{i\theta}, \quad |\xi|=1 . \quad (24)$$

We must choose $\mathrm{Im}\xi<0$, for, in this case, according to (22), $(\Omega^{-1})_{00}$, $(\Omega^{-1})_{11}$, etc., will have a negative imaginary part, corresponding to the correct analytic continuation, g^+.

If $t=\cos\theta$, for $t\to t+i\epsilon$, $\theta\to\theta'=\theta+i\eta$

$$t^+\equiv t+i\epsilon=\cos(\theta+i\eta)=\cos\theta\cosh\eta-i\sin\theta\sinh\eta , \quad (25)$$

then $\eta > 0$ if $\sin\theta < 0$ and

$$\xi = e^{i\theta'} = e^{i(\theta + i\eta)} = e^{i\theta} e^{-\eta} \ . \tag{26}$$

For ξ real, we must choose the solution $|\xi| < 1$, to which the continued fraction converges[12] and it can be immediately verified that when $t \to t + i\epsilon$, $\xi \to \xi - i\zeta$, with $\zeta > 0$.

Figure 1 represents the mapping $t \to \xi(t)$ on the complex ξ plane, where the particular branch has been chosen for which $|\xi(t + i\epsilon)| < 1$ and $\mathrm{Im}\xi(t + i\epsilon) < 0$.

The physical meaning of the parameter ξ can be visualized by considering one of the unperturbed equations (7) for a nondiagonal element $(\Omega g)_{nl}, n \neq l$ for $l \geq 3$:

$$g_{n-1,l} + 2t g_{n,l} + g_{n+1,l} = 0 \ . \tag{27}$$

If we call

$$g_{n,l} \equiv \mathrm{const}\, x_n \ , \tag{28}$$

where the constant factor depends on l, Eq. (27) can be rewritten as

$$x_{n-1} + 2t x_n + x_{n+1} = 0 \ , \tag{29}$$

with solutions

$$x_n = A \rho^n \ , \tag{30}$$

if ρ satisfies

$$(\rho + \rho^{-1}) + 2t = 0 \ . \tag{31a}$$

Comparing Eq. (31a) with Eq. (21) we see that

$$\rho = -\xi \ . \tag{31b}$$

The quantities x_n are the amplitudes of the eigenvectors of $\underline{H}^{\mathrm{eff}}$ at the plane n, since Eq. (29) can be recognized as the eigenvalue equation

$$(\underline{H}^{\mathrm{eff}} - \mathbb{1}\nu)\vec{x} = 0, \quad \vec{x} = (x_0, x_1, \ldots) \ ,$$

for fixed $\vec{k}_{\parallel}$.

The relations (28), (30), and (31b) imply

$$g_{n+1,l}(\vec{k}_{\parallel}, \omega) = \rho(\vec{k}_{\parallel}, \omega) g_{n,l}(\vec{k}_{\parallel}, \omega) = -\xi(\vec{k}_{\parallel}, \omega) g_{n,l}(\vec{k}_{\parallel}, \omega) \ . \tag{32}$$

We see that $\rho(\vec{k}_{\parallel}, \omega)$ is the transfer matrix for this case.

Let us now return to Eqs. (7a) and (7b) for the Green matrix $\underline{g}$ and observe that the poles of g coincide with the zeros of $\det\underline{\Omega}$ [defined in Eq. (9)].

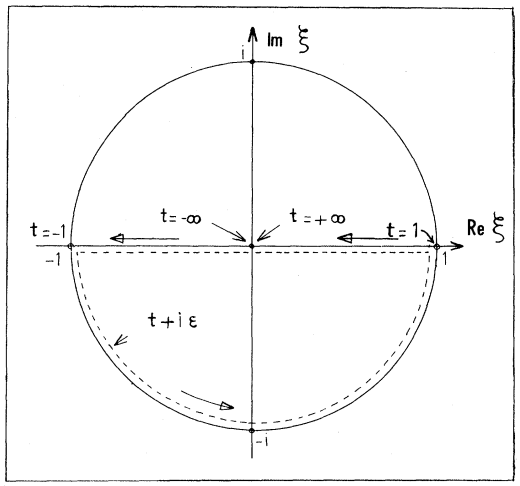

FIG. 1. The mapping $\xi = t \pm (t^2 - 1)^{1/2}$. We show the branch corresponding to the analytic continuation of t in the upper half-plane. The lower semicircumference is the image in the complex ξ plane of the branch cut $-1 \leq t \leq 1$ where the continuum lies. Long arrows indicate the sense in which ξ travels along its trajectory in the lower half-circumference as t varies in the whole real axis $-\infty < t < \infty$.

$g_{n,l}$ for all n and l can be written as the ratio of two polynomials. The diagonal elements of $\underline{g}$, in particular, which are the only ones we shall need to evaluate explicitly, can be expressed as

$$g_{ll}(\xi, \vec{k}_{\parallel}) = \frac{N_l(\xi, \vec{k}_{\parallel})}{D(\xi, \vec{k}_{\parallel})} \ , \tag{33}$$

where $D(\xi, \vec{k}_{\parallel})$ does not depend on l. For complex ξ, g^+ has a branch cut along the semicircumference $|\xi| = 1$ in the lower half plane, as shown in Fig. 1. For real $\xi = \xi_s$, a real root of $D(\xi, \vec{k}_{\parallel}) = 0$, we eliminate $2t$ in terms of ξ from Eq. (21), and substitute in Eq. (11) to obtain the frequency of a surface magnon as

$$v_s(\vec{k}_{\parallel}) = \xi_s + \xi_s^{-1} + 2 + 4[1 - \gamma_0(\vec{k}_{\parallel})] \ . \tag{34}$$

In Sec. III we describe the results obtained for the dispersion relation (34), for different magnon branches and different crystal structures.

In order to evaluate the magnetization, we require the equal-time correlation function $\langle S_n^- S_n^+ \rangle$. This can be obtained in terms of the Green functions (2) as[5]

$$\langle S_n^- S_n^+ \rangle = \lim_{\epsilon \to 0^+} i \int d(\hbar\omega) \frac{\langle\langle S_n^+; S_n^- \rangle\rangle_{E - \hbar\omega + i\epsilon} - \langle\langle S_n^+; S_n^- \rangle\rangle_{E - \hbar\omega - i\epsilon}}{\exp(\hbar\beta\omega) - 1} \ . \tag{35}$$

For the particular case $S = \frac{1}{2}$, we have

$$\langle S_n^- S_n^+ \rangle = \frac{\hbar^2}{2} - \hbar \langle S_n^z \rangle \ . \tag{36}$$

Then, in terms of $\tilde{G}$ defined in Eq. (5),

$$\frac{\hbar^2}{2}-\hbar\langle S_n^z\rangle=-\lim_{\epsilon\to 0^+}2\int d(\hbar\omega)\frac{a^2}{4\pi^2}\int d^2\vec{k}_{\parallel}\,\mathrm{Im}\tilde{G}_{nn}(\vec{k}_{\parallel},\omega+i\epsilon)[\exp(\hbar\beta\omega)-1]^{-1}\ . \tag{37}$$

For a general value of S we use a result due to Hewson and Ter Haar,[13] for the case of an infinite antiferromagnet:

$$\langle S_{\pm}^z\rangle=\frac{[S-\psi_{\pm}(S)][1+\psi_{\pm}(S)]^{2S+1}+[S+1+\psi_{\pm}(S)]^{2S+1}}{[1+\psi_{\pm}(S)]^{2S+1}-[\psi_{\pm}(S)]^{2S+1}}\ , \tag{38}$$

where

$$\psi_{\pm}(S)=-2\int_{-\infty}^{\infty}\mathrm{Im}G_{l(\pm),l(\pm)}(\omega+i\epsilon)[\exp(\hbar\beta\omega)-1]^{-1}d(\hbar\omega)\ . \tag{39}$$

The labels $(\pm)$ in that particular case referred to the up or down sublattice. In order to generalize (38) to apply for the case of a system with a magnetization varying from plane to plane parallel to the surface, we must extend the formulas to include an infinite number of sublattices, each of which is in fact one crystal plane. The integration over three-dimensional $\vec{k}$ space must be substituted by an integration over the two-dimensional $\vec{k}_{\parallel}$ space, appropriate to the particular family of planes parallel to the surface and the label $\pm$ must be substituted by the corresponding plane index, so that we have one function $\psi_n(S)$ for each plane in the semi-infinite system.

In our case, then

$$\langle S_n^z\rangle=\frac{[S-\psi_n(S)][1+\psi_n(S)]^{2S+1}+[S+1+\psi_n(S)][\psi_n(S)]^{2S+1}}{[1+\psi_n(S)]^{2S+1}-[\psi_n(S)]^{2S+1}}\ , \tag{40}$$

where $\psi_n(S)$ is

$$\psi_n(S)=-\frac{1}{\pi}\int dt\frac{a^2}{4\pi^2}\int d^2\vec{k}_{\parallel}\,\mathrm{Im}(\Omega^{-1})_{nn}(t+i\epsilon,\vec{k}_{\parallel})[\exp(\alpha_0(T,S)\{2t+2+4[1-\gamma_0(\vec{k}_{\parallel})]\})-1]^{-1}\ , \tag{41}$$

$$\alpha_0(T,S)=\frac{2\hbar I\langle S_{\mathrm{vol}}^z\rangle}{kT}\ . \tag{42}$$

We now refer to Fig. 1, in order to evaluate the integral in (41); t varies from $-\infty$ to ∞ as the frequency ω does. In the range $-\infty<t<-1$ and $1<t<\infty$, ξ is real and varies from -1 to $+1$. Then in terms of the real roots $\{\xi_\alpha\}$ of $D(\xi_\alpha)=0$,

$$\mathrm{Im}(\Omega^{-1})_{nn}(\vec{k}_{\parallel},\xi-i0^+)=-\pi\sum_{\alpha}\delta(\xi-\xi_\alpha)\frac{N_n(\xi_\alpha)}{D'(\xi_\alpha)}\ . \tag{43}$$

Substituting (43) into (41) for $|t|>1$, we obtain the contribution to the spin deviation from the discrete spectrum of surface modes, denoted with the index α in (43). The integral

$$\int_{-1}^{1}dt\int d^2k_{\parallel}\cdots\ ,$$

in (41) runs over the range where the Green function has a branch cut, it being the contribution to the spin deviation from the continuum spectrum of bulk excitations.

Equation (40) for different n will give a set of self-consistent equations which, for $S=\frac{1}{2}$, can be written as[7]

$$\langle S_n^z\rangle=\frac{(\frac{1}{2})\hbar}{1+2\psi_n(\frac{1}{2})}\ . \tag{44}$$

B. fcc ferromagnet

We consider a (111) surface. The basis vectors are chosen as

$$\vec{A}_1=\frac{a}{2}(1,0,\bar{1}),\quad \vec{A}_2=\frac{a}{2}(0,1,\bar{1})\ ,\qquad \vec{A}_3=\frac{a}{2}(1,1,0)\ . \tag{45}$$

The reciprocal vectors are

$$\vec{B}_1=\frac{2\pi}{a}(1,\bar{1},\bar{1}),\quad \vec{B}_2=\frac{2\pi}{a}(\bar{1},1,\bar{1})\ ,\qquad \vec{B}_3=\frac{2\pi}{a}(1,1,1)\ . \tag{46}$$

A general $\vec{k}$ vector will be written as

$$\vec{k}=\sum_{i=1}^{3}k_i\vec{B}_i \tag{47}$$

or as $\vec{k}=(\vec{k}_{\parallel},k_3)$. Therefore a vector $\vec{k}_{\parallel}=(k_1,k_2)$ describes wave propagation parallel to the plane (111) although it is not itself parallel to the plane.

In order to obtain the equation of motion for the Green function in this case it is convenient to generalize the Fourier transform with respect to $\vec{f}_{\parallel}$, $\vec{g}_{\parallel}$ by including a phase change from one plane to the next away from the surface[14]:

$$G_{fg}(\omega)=\frac{1}{N_S}\sum_{\vec{k}_{\parallel}} G_{f_3g_3}(\vec{k}_{\parallel},\omega) \times\exp[i\vec{k}_{\parallel}(\vec{f}_{\parallel}-\vec{g}_{\parallel})+i\psi(\vec{k}_{\parallel})(f_3-g_3)] , \tag{48}$$

$$I_{fg}=\frac{1}{N_S}\sum_{\vec{k}_{\parallel}} \tilde{I}_{f_3g_3}(\vec{k}_{\parallel}) \times\exp[i\vec{k}_{\parallel}(\vec{f}_{\parallel}-\vec{g}_{\parallel})+i\psi(\vec{k}_{\parallel})(f_3-g_3)] , \tag{49}$$

$\psi(\vec{k}_{\parallel})$ is the phase of the structure factor h, defined as

$$h\equiv\phi e^{i\psi}=\tfrac{1}{3}[1+\exp(2\pi ik_1)+\exp(2\pi ik_2)] ;$$

$$\phi^2=\tfrac{1}{9}(3+2\{[\cos2\pi(k_1-k_2)]+\cos2\pi k_1+\cos2\pi k_2\})$$

$$\tan\psi(\vec{k}_{\parallel})=(\sin2\pi k_1+\sin2\pi k_2)\times(1+\cos2\pi k_1+\cos2\pi k_2)^{-1} .$$

Substitution of transforms (48) and (49) into (4) gives just an equation equivalent to (7), and the introduction of the phase $\psi(\vec{k}_{\parallel})(f_3-g_3)$ makes the nondiagonal matrix elements of $\underline{H}^{\rm eff}$ real.

The exchange constants for bonds linking spins on the (111) surface plane and between the surface and the next inner plane are eventually assumed different from the volume constants. We define

$$\left.\begin{aligned}&\tfrac{1}{3}\alpha_{00}=2-\sigma_1\epsilon_{\perp}+4(1-\epsilon_{\parallel}\sigma_0)[1-\gamma_1(\vec{k}_{\parallel})]\\&\tfrac{1}{3}\alpha_{11}=1-\sigma_0\epsilon_{\perp}+4(1-\sigma_1)[1-\gamma_1(\vec{k}_{\parallel})]\\&\tfrac{1}{3}\alpha_{22}=1-\sigma_1\\&\gamma_1(\vec{k}_{\parallel})=1-\tfrac{3}{4}(1-\phi^2)\end{aligned}\right\} . \tag{50}$$

The matrix $\underline{\Omega}=\nu\mathbb{1}-\underline{H}^{\rm eff}$ can be written as

$$\underline{\Omega}=\begin{pmatrix}2t+\alpha_{00} & 3\phi\epsilon_{\perp}\sigma_0 & 0 & 0 & 0 & \cdot & \cdot & \cdot\\ 3\phi\epsilon_{\perp}\sigma_1 & 2t+\alpha_{11} & 3\phi\sigma_1 & 0 & 0 & 0 & \cdot & \cdot\\ 0 & 3\phi & 2t+\alpha_{22} & 3\phi & 0 & 0 & \cdot & \cdot\\ 0 & 0 & 3\phi & 2t & 3\phi & 0 & \cdot & \cdot\\ 0 & 0 & 0 & 3\phi & 2t & 3\phi & \cdot & \cdot\\ \cdot & \cdot & \cdot & \cdot & \cdot & \cdot & \cdot & \cdot\\ \cdot & \cdot & \cdot & \cdot & \cdot & \cdot & \cdot & \cdot\\ \cdot & \cdot & \cdot & \cdot & \cdot & \cdot & \cdot & \cdot\end{pmatrix} . \tag{51}$$

It turns out convenient to divide all elements of $\underline{\Omega}$ by $3\phi(\vec{k}_{\parallel})$, so that in terms of the new variables $t'=t/3\phi$, $\alpha'_{00}=\alpha_{00}/3\phi$, $\alpha'_{11}=\alpha_{11}/3\phi$, etc., we obtain a matrix $\underline{\Omega}'$ which has the same structure as $\underline{\Omega}$ of Eq. (7) for the sc lattice. In particular, making the substitutions $t'\to t$, $\alpha'_{00}\to\alpha_{00}$, etc., to simplify the notation we have

$$(\Omega^{-1})_{00}=\left(\frac{1}{3\phi}\right)\cfrac{1}{2t+\alpha_{00}-\cfrac{\beta_{01}\beta_{10}}{2t+\alpha_{11}-\cfrac{\beta_{12}\beta_{21}}{2t+\alpha_{22}-\xi}}} . \tag{52}$$

In terms of the new variable t,

$$\nu=3[2\phi t+2+4(1-\gamma_1(\vec{k}_{\parallel})] , \tag{53}$$

and the self-consistent system of equations for σ_n as defined in (8b) is the same as (40) and (41) with the argument of the Bose function modified to

$$\alpha_1(T,S)[2\phi t+2+4(1-\gamma_1(\vec{k}_{\parallel})] , \tag{54}$$

where

$$\alpha_1(T,S)=3\alpha_0(T,S) . \tag{55}$$

III. RESULTS FOR THE MAGNETIZATION AND THE DISPERSION RELATIONS

We show in Figs. 2 and 3 the curves for $\langle S_0^z\rangle$ vs T for different values of $\epsilon_{\perp}$, with $\epsilon_{\parallel}=1$. Figure 4 shows the dispersion relations of the different surface magnon branches for the fcc lattice (the corresponding results for the sc lattice were already published in Ref. 6). The limits of the continuum are also indicated in Fig. 4. As a general trend, we note that increasing T is equivalent to decreasing $\epsilon_{\perp}$ and $\epsilon_{\parallel}$, since in both cases the total field on surface spins decreases.

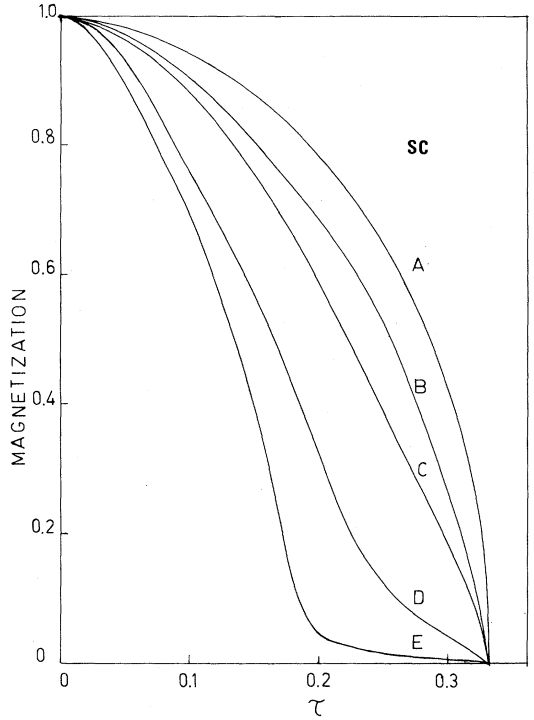

FIG. 2. Surface magnetization for the sc lattice as a function of temperature: $\tau = kT/(6I\hbar^2)$. The bulk magnetization is also shown. The critical temperature in our units is $\tau_c = 0.33$. The surface is a (100) plane; $S = \frac{1}{2}$. A: σ_v; $\epsilon_{\parallel} = 1$, $\epsilon_{\perp} = 1$ (B), 0.5 (C), 0.1 (D), and 0.01 (E).

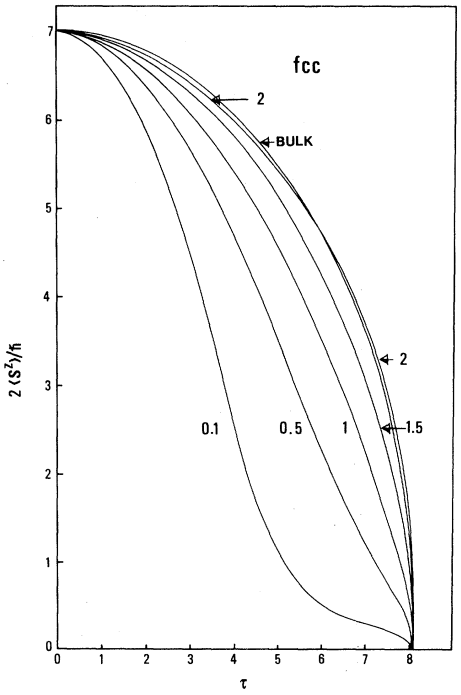

FIG. 3. Surface magnetization for the fcc lattice with a (111) surface as a function of reduced temperature $\tau = kT/(12I\hbar^2)$ and $S = \frac{7}{2}$. The reduced critical temperature is $\tau_c = 8.04$, for $\epsilon_{\parallel} = 1$ and the indicated values of $\epsilon_{\perp}$.

As T increases, therefore, acoustic surface branches tend to appear or to become more separated from the continuum from below, while on the contrary, optical surface branches tend to disappear, or to approach the upper limit of the continuum. $\epsilon_{\perp} \gtrless 1$ favors (optical, acoustic) branches, respectively. As it has already been found earlier[6] for the sc lattice, the bulk critical temperature T_c also drives the transition to the paramagnetic phase at the surface, in fcc case (Fig. 3).

From Figs. 2 and 3 we observe that as $\epsilon_{\perp}$ decreases, the surface shows a tendency to cross over to the two-dimensional behavior $T_c = 0$.[6]

As regards the spatial variation of the magnetization (Fig. 5) in the present paper we have limited ourselves, for simplicity, to consider only variations of $\langle S_n^z \rangle$ over the first two planes.

The results, which coincide qualitatively with those obtained previously for the simple cubic case,[6] indicate that the convergence to the bulk magnetization is very fast indeed, supporting our assumption that only the first few planes would differ appreciably from the bulk. Other results, obtained with Monte Carlo calculations, indicate that a small deviation from the bulk can extend to greater distances.[15] We can, however, be confident that this correction will

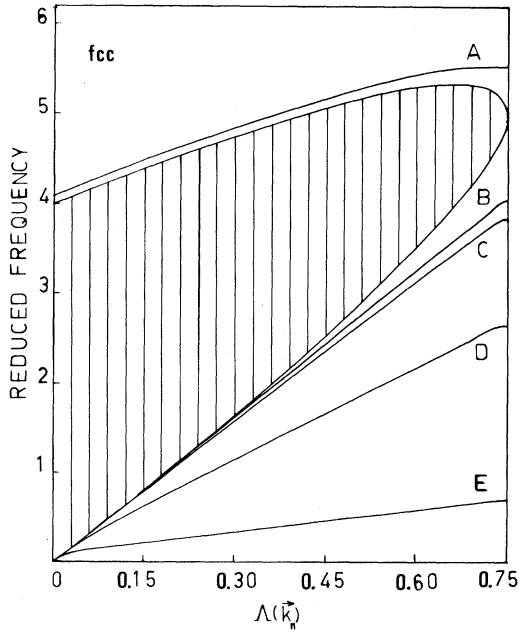

FIG. 4. Dispersion relations for surface magnons in the fcc lattice. The dashed region is the bulk continuum. Along the horizontal axis is plotted $\Lambda(\vec{k}_{\parallel}) = 1 - \gamma_1(\vec{k}_{\parallel})$ [see Eq. (53)]. The different curves correspond respectively to A: $\tau = 2$, $\epsilon_{\perp} = 1.5$; B: $\tau = 2$, $\epsilon_{\perp} = 0.1$; C: $\tau = 5$, $\epsilon_{\perp} = 0.1$; D: $\tau = 2$; $\epsilon_{\perp} = 0.1$; E: $\tau = 5$, $\epsilon_{\perp} = 0.1$; and $\epsilon_{\parallel} = 1$, $S = \frac{7}{2}$.

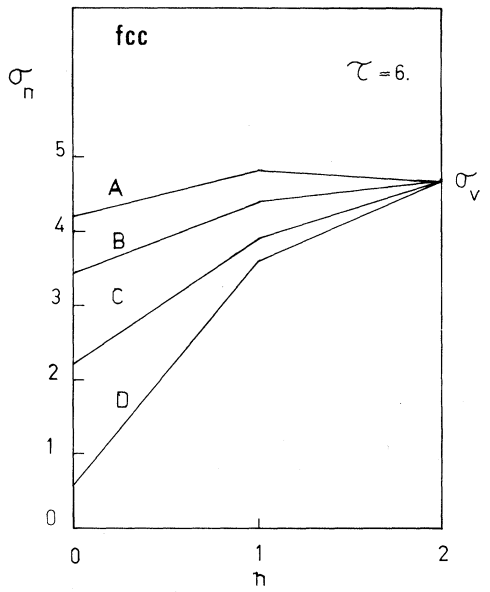

FIG. 5. Magnetization profile for the fcc lattice. $\tau=6$, $\epsilon_{\parallel}=1$, $\epsilon_{\perp}=1.5$ (A), 1 (B), 0.5 (C), 0.1 (D). $\sigma_n=2\langle S_n^z\rangle/\hbar$, $\sigma_v=2\langle S_{\text{vol}}^z\rangle/\hbar$, $S=\frac{7}{2}$.

affect our results by just a few percent after the second plane, since in two different calculations for the sc structure, involving, respectively, one and two altered planes, the surface magnetization differed by only 15%.[6]

It must be remared that as $\epsilon_{\perp}$ increases above 1.5, the magnetization of the second plane becomes slightly greater than the bulk value at high T. This result may be due to the restriction to only two varied planes. Also, the critical behavior of $\langle S_0^z\rangle$ for $T \lesssim T_c$ is presumably dependent on this approximation, since the effect of imposing $\sigma_2=1$ is to increase artificially the self-consistent values $\langle S_0^z\rangle$ and $\langle S_1^z\rangle$.

Further work to extend the present calculations to $\sigma_2 \neq 1$ is already in progress.

We estimate that the present results will be unaltered for $T \lesssim 0.9T_c$ and for $\epsilon_{\perp} \lesssim 2.0$.

IV. INELASTIC SCATTERING OF LOW-ENERGY ELECTRONS

The interaction between the incident electrons and the spin lattice is described by a contact potential introduced by de Gennes and Friedel[11]:

$$V(\vec{r}) = \left(\frac{G\Omega_c}{2}\right)\vec{s}(\vec{r})\cdot\sum_{\vec{l}}\vec{S}_{\vec{l}}\rho(\vec{r}-\vec{l}) \quad , \tag{56}$$

where G is the coupling constant, Ω_c is the volume of the unitary cell, $\vec{S}(\vec{r})$ the spin operator of the incident electron, $\vec{S}_{\vec{l}}$ the spin operator in the $\vec{l}$ position of the lattice, and $\rho(\vec{r})$ the electronic spin density of the ion.

The differential cross section in the Born approximation is

$$\frac{d^2\sigma}{dE\,d\Omega} = \frac{k'}{k}\left(\frac{m}{2\pi}\right)^2 \sum_{i,f,s,s'} |\langle \vec{k}'s'f|V|\vec{k}si\rangle|^2 W(i)P(s)\delta(E-E_i+E_f) \quad , \tag{57}$$

m is the free-electron mass; $|\vec{k},s\rangle$ the incident-electron state; $|\vec{k}',s'\rangle$ the scattered-electron state; i and f denote, respectively, the initial and final states of the target. $W(i)=e^{-\beta E_i}/\mathrm{Tr}(e^{-\beta H})$ is the probability of finding the magnetic system in the initial state i, and $P(s)$ is the probability that an incoming electron has spin s. We assume small energy transfer E, so $k' \simeq k$. The wave function of the incident electron is assumed of the form[3]

$$\varphi_{\vec{k}_{\parallel},k_3}(\vec{r}) = \exp(-i\vec{k}_{\parallel}\cdot\vec{r}_{\parallel})f_{k_3}(z) \quad . \tag{58}$$

Let us calculate the matrix element

$$\left\langle \vec{k}',s',f\left|\sum_{\vec{l}}\vec{s}\cdot\vec{S}_{\vec{l}}\rho(\vec{r}-\vec{l})\right|\vec{k},s,i\right\rangle \quad . \tag{59}$$

The lth term of the sum is ($\alpha=+,-,z$):

$$\langle \vec{k}'s'f|s^{\alpha}S_{\vec{l}}^{\alpha}\rho(\vec{r}-\vec{l})|\vec{k},s,i\rangle = \langle f|S_{\vec{l}}^{\alpha}|i\rangle\langle s'|s^{\alpha}|s\rangle\int d\vec{r}\,\varphi^*_{\vec{k}'_{\parallel},k_3'}(\vec{r})\rho(\vec{r}-\vec{l})\varphi_{\vec{k}_{\parallel},k_3}(\vec{r}) \quad . \tag{60}$$

We call

$$\langle s'|s^{\alpha}|s\rangle = \lambda^{\alpha}_{s's} \quad . \tag{61}$$

Now we calculate the integral

$$\int d\vec{r}\,\varphi_{\vec{k}'_{\parallel},k_3'}(\vec{r})\rho(\vec{r}-\vec{l})\varphi_{\vec{k}_{\parallel},k_3}(\vec{r}) = \exp(i\Delta\vec{K}_{\parallel}\cdot\vec{l}_{\parallel})\gamma_n(\Delta\vec{k}_{\parallel},k_3',k_3) \quad , \tag{62a}$$

where $\Delta\vec{k}_{\parallel}=\vec{k}'_{\parallel}-\vec{k}_{\parallel}$ and

$$\gamma_n(\Delta\vec{k}_{\parallel},k_3',k_3)=\int d\vec{r}'\, f_{k_3'}(r_3'+n)f_{k_3}(r_3'+n)\,\rho(\vec{r}')\exp(i\Delta\vec{k}_{\parallel}\cdot\vec{r}_{\parallel}) \quad . \tag{62b}$$

Here, we assume for simplicity that the electron wave functions do not depend on spin. Then (57) becomes

$$\left(\frac{d^2\sigma}{dE\,d\Omega}\right)_{s'}=\left(\frac{m}{2\pi}\right)^2\frac{G\Omega_0}{2}\sum_{i,f,s,\vec{\Gamma}_n,\vec{\Gamma}_{\parallel},\vec{\Gamma}'_{\parallel},n,n'} p(s)\gamma_n^*\gamma_{n'}\exp(-i\Delta\vec{k}_{\parallel}\cdot\vec{\Gamma}_{\parallel})\lambda^{\alpha}_{s's}\langle f|S^{\alpha}_{\vec{\Gamma}}|i\rangle\exp(i\Delta\vec{k}_{\parallel}\cdot\vec{\Gamma}'_{\parallel})(\lambda^{\beta}_{s's})^*$$

$$\times\langle f|S^{\beta}_{\vec{\Gamma}'}|i\rangle^*\frac{e^{-\beta Ei}}{z}\delta(E+E_f-E_i) \quad . \tag{63}$$

The terms in (63) involving S_n^z are substituted in the RPA by the averages $S_n^z\to\langle S_n^z\rangle$ and are subsequently independent on time, so they do not contribute to the inelastic scattering. They will be excluded in what follows.

We introduce the mixed local-Bloch spin operators

$$S^{+}_{\Delta\vec{k}_{\parallel},n}=\sum_{\vec{\Gamma}_{\parallel}}\exp(i\Delta\vec{k}_{\parallel}\cdot\vec{\Gamma}_{\parallel})S^{\pm}_{\vec{\Gamma}_{\parallel},n} \quad ,$$
$$S^{-}_{\Delta\vec{k}_{\parallel},n}=(S^{+}_{\Delta\vec{k}_{\parallel},n})^{\dagger} \quad . \tag{64}$$

Due to angular momentum conservation the part of (63) which contributes to the matrix element (59) is

$$\tfrac{1}{2}(s^{+}S^{-}_{\Delta\vec{k}_{\parallel},n}+s^{-}S^{+}_{\Delta\vec{k}_{\parallel},n}) \quad . \tag{65}$$

Substituting (65) into (63) and writing

$$\delta(x)=\frac{1}{2\pi}\int_{-\infty}^{\infty}dt\,e^{ixt}$$

we find

$$\left(\frac{d^2\sigma}{dE\,d\Omega}\right)^{\text{inel}}_{s'}=\left(\frac{m}{2\pi}\right)^2\frac{G\Omega_c}{2}\sum_{s,n,n'}P(s)\frac{\gamma_n^*\gamma_{n'}}{4}\left(\frac{\lambda^{+}_{s's}\lambda^{-}_{ss'}}{2\pi}\int_{-\infty}^{\infty}dt\,e^{iEt}\langle S^{-}_{\Delta\vec{k}_{\parallel},n}(0)S^{+}_{\Delta\vec{k}_{\parallel},n'}(t)\rangle\frac{\lambda^{-}_{s's}\lambda^{\dagger}_{ss'}}{2\pi}\right.$$

$$\left.\times\int_{-\infty}^{\infty}dt\,e^{iEt}\langle S^{+}_{\Delta\vec{k}_{\parallel},n}(0)S^{-}_{\Delta\vec{k}_{\parallel},n'}(t)\rangle\right) \quad . \tag{66}$$

We shall assume that electrons do not penetrate farther than the first plane,[3] $n=0$.

The correlation functions $\langle S^{\pm}_{\Delta\vec{k}_{\parallel},n}(0)S^{\mp}_{\Delta\vec{k}_{\parallel},n}(t)\rangle$ can be related to the Green functions

$$\int_{-\infty}^{\infty}\langle S^{\mp}_{\Delta\vec{k}_{\parallel},n}(0)S^{\pm}_{\Delta\vec{k}_{\parallel},n'}(t)\rangle e^{iEt}\frac{dt}{2\pi}=-2\,\text{Im}\langle\langle S^{\pm}_{\Delta\vec{k}_{\parallel},n};S^{\mp}_{\Delta\vec{k}_{\parallel},n}\rangle\rangle_E^{+}[\exp(\beta E)-1]^{-1} \quad . \tag{67}$$

We assume that $P(s)$, the polarization fraction of the incident electrons, has the form

$$P(s)=\begin{cases}p, & s=\uparrow\\ 1-p, & s=\downarrow\end{cases} \quad . \tag{68}$$

The matrix elements $\langle s|\lambda^{\alpha}|s'\rangle$ are

$$\lambda^{+}_{\uparrow\downarrow}=\lambda^{-}_{\downarrow\uparrow}=1 \quad .$$

We assume $\uparrow$ is parallel to the magnetization. For $s'=\uparrow$, corresponding to absorption of energy by the electron beam,

$$\left(\frac{d^2\sigma}{dE\,d\Omega}\right)^{\text{inel}}_{\uparrow}=-\left(\frac{m}{2\pi}\right)^2\frac{G\Omega_c}{4}|\gamma|^2 p\,\text{Im}\langle\langle S^{+}_{\Delta\vec{k}_{\parallel},0};S^{-}_{\Delta\vec{k}_{\parallel},0}\rangle\rangle_E^{+}B(E) \quad . \tag{69}$$

For $s'=\downarrow$, corresponding to a loss of energy by the electrons

$$\left(\frac{d^2\sigma}{dE\,d\Omega}\right)^{\text{inel}}=-\left(\frac{m}{2\pi}\right)^2\left(\frac{G\Omega_c}{4}\right)|\gamma|^2(1-p)\text{Im}\langle\langle S^{+}_{\Delta\vec{k}_{\parallel},0};S^{-}_{\Delta\vec{k}_{\parallel},0}\rangle\rangle_E^{-}[1-B(-E)] \quad , \tag{70}$$

where $B(E)=(e^{\beta E}-1)^{-1}$.

V. RESULTS FOR THE SCATTERING CROSS SECTION

Our results show that the spectral density of magnon states at the surface plane, which is the main ingredient entering expressions (69) and (70) for the inelastic scattering cross section, is strongly dependent upon the surface parameters. Curves for $d^2\sigma/(dE\,d\Omega)$ (Figs. 6 and 7) at small momentum transfer $|\Delta\vec{k}_{\parallel}| \sim 0$, and for $\epsilon_{\perp} < 1$ show just a strong maximum near the low-energy edge of the continuum and as energy increases, they decrease until near the upper edge $(t=1)\mathrm{Im}g_{00}$ vanishes like $(1-t)^{1/2}$. For $\epsilon_{\perp} > 1$, on the contrary, we observe that, besides the strong maximum close to the lower-energy edge, there appears another peak at the upper edge.

It is not difficult to interpret this qualitative behavior of the local density of magnons. For $\epsilon_{\perp} < 1$, as Fig. 4 shows, there is an acoustic surface magnon branch, of energy very close to the lower edge of the continuum. This shows itself as a strong surface resonance in the bulk magnon wave functions of low energy at $n=0$, and as a concentration of bulk states therein. As $\epsilon_{\perp}$ increases, we still find, as can be seen in Figs. 6 and 7 for $\epsilon_{\perp}=1.5$, an acoustic surface magnon, but at the same time an optical surface magnon branch appears at energies above the continuum, and this produces a similar resonant effect upon the bulk states with energy close to the upper continuum edge, which manifests itself in the smaller peak at the high-energy side.

The effect of temperature, apart from an overall scaling due to the bulk magnetization factor in $\mathrm{Im}g_{00}$ [Eq. (7b)] is to reduce appreciably the surface magnetization as compared to the bulk value, as discussed in Sec. II, and shown in Figs. 2 and 3. This reduction of $\langle S_{\vec{0}}^{z} \rangle$ as T increases, is in a way equivalent to a reduction both of $\epsilon_{\perp}$ *and* $\epsilon_{\parallel}$, and in this respect the present results are different from those of Harriague *et al.*[9] for the bcc ferromagnet at $T \approx 0$, where only $\epsilon_{\perp}$ was modified.

Another obvious effect of a finite T is the possibility of magnon absorption by the incident electron.

The calculations of Sec. III are performed with a view to interpreting a scattering experiment with spin-polarized electrons.

The elastic scattering differential cross section will depend, approximately (that is, within RPA) upon $(\langle S_{\vec{0}}^{z} \rangle)^2$ as we mentioned in Sec. IV. This fact has been applied by Wolfram *et al.*[16] to obtain experimentally the surface magnetization of antiferromagnetic NiO. Therefore, through simultaneous measurement of the elastic and inelastic spin-polarized scattering cross section, one can obtain $\langle S_{\vec{0}}^{z} \rangle$ and the local spectral density of magnons, $\mathrm{Im}g_{00}(\Delta\vec{k}_{\parallel}, \omega)$.

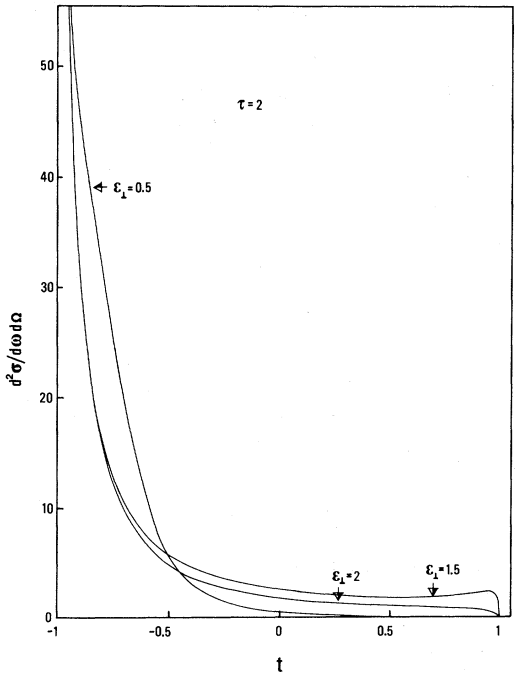

FIG. 6. Plot of the differential scattering cross section for inelastic scattering of slow electrons for magnon emission. All dimensional and kinematical factors have been omitted, so that the quantity along the vertical axis is $\mathrm{Im}g_{00}[1+B(-E)]$ for the fcc lattice for $\tau=2$, $\epsilon_{\perp}=0.5$, 1.5, and 2.0, $\epsilon_{\parallel}=1$, $S=\frac{7}{2}$.

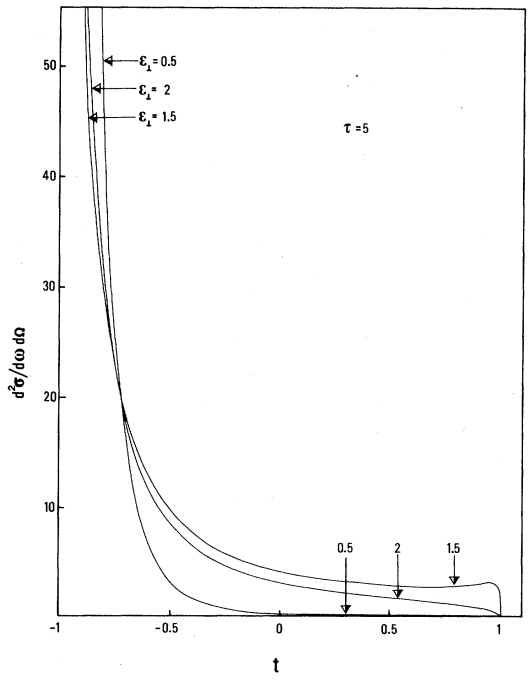

FIG. 7. The same as in Fig. 6 for $\tau=5$, $\epsilon_{\perp}=0.5$, 1.5, and 2.0, $\epsilon_{\parallel}=1$.

VI. CONCLUSIONS

This paper extends a series of previous works on the spectrum of surface magnetic excitations based on the Heisenberg exchange model to the whole range of temperatures up to the critical temperature, incorporating into the formalism a self-consistent procedure for the calculation of the nonuniform magnetization which is relatively simple and can be applied with small modifications to a variety of situations. The limitations of the present treatment, particularly the simplification that only two planes were assumed to be different from the bulk, can easily be overcome in principle and work to generalize the formalism to an arbitrary number of varied planes is already in progress. Other shortcomings of the present formalism are inherent to the RPA and must be overcome by performing a better treatment of the longitudinal fluctuations, that is by considering the effect of the difference $S_n^z - \langle S_n^z \rangle$ and eventually also the effect of finite lifetime upon the magnon states. Some of these improvements ought to be definitely incorporated into the theory before the critical behavior of the surface magnetization can be more confidently described. Our results indicate, at any rate, that the critical exponent of the surface magnetization is certainly less than one, and that it seems to depend on $\epsilon_\perp$. These conclusions, provisional as they are on the basis of the preceding criticisms, agree qualitatively with the Monte Carlo calculations of Binder and Hohenberg,[15] with renormalization-group calculations by several authors[17] and are also consistent with recent experimental measurements by Alvarado *et al.*[18] of the critical exponent of the (100) surface magnetization of Ni.

Another conclusion of our work is that by measuring the elastic and inelastic differential cross section for low energy, spin-polarized electrons, a great deal of information can be gathered on the exchange interactions at the surface plane of insulating ferromagnets, and we expect that formulas (69) and (70) of Sec. IV provide a useful model for interpreting such experiments. In particular, the effect of changing the temperature and/or the surface parameters can be traced to the appearance of resonance peaks in the differential scattering cross sections, which, in turn, is simply related to the surface spectral distribution function of the magnetic excitations.

ACKNOWLEDGMENTS

During the whole course of this work, we have enjoyed invaluable advice on numerical computation methods from Professor Sergio S. Makler and many stimulating discussions with Professor Enrique V. Anda and Professor José E. Ure. We acknowledge also several useful comments from Professor Leo Falicov. Special thanks are due to Professor A. Baldereschi for having provided us with the necessary data for applying a fast numerical integration method in $\vec{k}$ space. Professor Fernando A. de Oliveira we thank for his careful reading of the manuscript. We are grateful to Professor Abdus Salam, the International Atomic Energy Agency, and UNESCO for hospitality at the International Centre for Theoretical Physics, Trieste. The present work has been partially supported by Conselho Nacional de Desenvolvimento Científico e Tecnológico (CNPq) and Financiadora de Estudos e Projetos (FINEP) of Brazil, and by Scuola Internazionale Superiore di Studi Avanzati (SISSA), Trieste.

---

*Permanent address: Instituto de Fisica, Universidade Federal Fluminense, Caixa Postal 296, 24.210 Niteroi, RJ, Brazil.

[1]D. T. Pierce and Felix Meier, Phys. Rev. B 13, 5484 (1976).

[2]G. P. Felcher, S. D. Bader, R. J. Celotta, D. T. Pierce, and G. C. Wang, in *Ordering in Two Dimensions,* edited by S. K. Sinha (Elsevier/North-Holland, Amsterdam, 1980).

[3]D. L. Mills, J. Phys. Chem. Solids 28, 2245 (1967).

[4]R. E. De Wames and T. Wolfram, Phys. Rev. 185, 720 (1969).

[5]D. N. Zubarev, Usp. Fiz. Nauk 71, 71 (1960) [Sov. Phys. Usp. 3, 320 (1960)].

[6]S. Selzer and N. Majlis, J. Magn. Magn. Mater. 15–18, 1905 (1980).

[7]R. A. Tahir-Kheli and D. Ter Haar, Phys. Rev. 127, 88 (1962).

[8]Diep-The-Hung, J.C.S. Levy, and O. Nagai, Phys. Status Solidi B 93, 351 (1979).

[9]S. Harriague, N. Majlis, S. A. Makler, and A. M. Olmedo, Phys. Status Solidi B 66, 377 (1974).

[10]X. Saldaña and J. S. Helman, Phys. Rev. B 16, 4978 (1977).

[11]P. G. De Gennes and J. Friedel, Phys. Chem. Solids 4, 71 (1958).

[12]H. S. Wall, *Analytic Theory of Continued Fractions* (Van Nostrand, New York, 1948).

[13]A. C. Hewson and D. Ter Haar, Physica (Utrecht) 30, 899 (1964).

[14]S. Harriague and N. Majlis, Int. J. Magn. 6, 269 (1974).

[15]K. Binder and P. C. Hohenberg, Phys. Rev. B 9, 2194 (1974).

[16]T. Wolfram, R. E. De Wames, W. F. Hall, and P. W. Palmberg, Surf. Sci. 28, 45 (1971).

[17]J. C. Le Guillou and J. Zinn-Justin, Phys. Rev. B 21, 3976 (1980); J. S. Reeve and A. J. Guttmann, Phys. Rev. Lett. 45, 1581 (1980).

[18]S. Alvarado, M. Campagna, and H. Gopster (unpublished).